



OPEN

# DNA barcodes for delineating *Clerodendrum* species of North East India

Barbi Gogoi<sup>1,2</sup>, S. B. Wann<sup>3</sup> & S. P. Saikia<sup>1</sup>✉

The diversified genus of *Clerodendrum* with its complex evolutionary history leads to taxonomic mystification. Unlike traditional taxonomic methods, DNA barcoding could be a promising tool for the identification and conservation of *Clerodendrum* species. This study was attempted to develop an efficient barcode locus in *Clerodendrum* species of North East India. We evaluated four barcode candidates (*ITS2*, *matK*, *rbcL*, *ycf1*) and its combinations in different *Clerodendrum* species. The reliability of barcodes to distinguish the species were calculated using genetic pairwise distances, intra- and inter-specific diversity, barcode gap, and phylogenetic tree-based methods. The results exemplify that *matK* posse's maximum number of variables and parsimony-informative sites (103/100), intra- ( $0.021 \pm 0.001$ ) and inter- ( $0.086 \pm 0.005$ ) specific divergences and species resolution rate (89.1%) followed by *ITS2*, *ycf1*, and *rbcL*. Among the combinatorial locus, *ITS2* + *matK* showed the best species discrimination with distinctive barcode gaps. Therefore, we tentatively suggest that the combination of *ITS2* + *matK* as core barcode for *Clerodendrum* and converted into quick response (QR) code. Hence, this finding indicates that DNA barcoding could provide consistent resources for species discrimination and resolve taxonomic controversies of the genus as well as set a preliminary assessment toward its biodiversity.

North East India is endowed with enormous biodiversity of flora and fauna. *Clerodendrum* is a large, complex, and diversified genus that encompasses well-established pharmacological properties and its importance of ethnomedical assets was reported in many indigenous systems of medicines<sup>1</sup>. Globally, 540 *Clerodendrum* species were distributed in tropical and sub-tropical regions that include small trees, shrubs, and herbs<sup>2</sup>. Approximately, 23 *Clerodendrum* species were found in India, while 18 species occur in North East India<sup>3</sup>. The family of *Clerodendrum* was moved from Verbenaceae to Lamiaceae based on circumscription of evolutionary boundaries through molecular evidences<sup>4</sup>. Based on morphological variations, authors classified the genus into distinctive subgenera like *Clerodendrum* and *Cyclonema*, also numerous species were described by more than one authors such as *C. floribundum* Hort and *C. floribundum* R.Br., *C. foetidum* Bunge and *C. foetidum* D.Don, etc.<sup>5,6</sup>. Therefore, DNA barcoding techniques could function as a molecular identifier for proper documentation and classification of *Clerodendrum*. DNA barcoding uses short standardized region of DNA sequence(s) (either nuclear or/and cytoplasmic genome) for rapid authentication of discrete species and cost-effective in nature<sup>7</sup>. Unlike animals, the mitochondrial genes were an unsuitable choice of barcode marker in plants due to its low nucleotide substitutions rates. Subsequently, numerous nuclear and plastid genes were leading the focus of researchers for identifying plant species<sup>8</sup>. So far, no consensus emerged as the universal barcode for land plants<sup>9</sup>. However, the multi-locus combination of barcode could enhance the potential discriminatory rates between closely related species<sup>10</sup>. To date, no authenticated report on the practice of DNA barcoding in *Clerodendrum* sp. was cited. In this study, we collected only 9 species of *Clerodendrum* from different locations of North East India, and the rest of the species were not encountered during the fieldwork as they were extremely rare and only known from a small number of locations.

The accessibility of DNA barcoding in its practical application was constrained due to its difficulty in retrieval of information via direct scanning of DNA sequences<sup>11</sup>. The DNA sequences contain long strings of characters

<sup>1</sup>Medicinal Aromatic and Economic Plants Group, Biological Sciences & Technology Division (BSTD), CSIR-North East Institute of Science & Technology, Jorhat 785006, Assam, India. <sup>2</sup>Academy of Scientific and Innovative Research (AcSIR), Ghaziabad 201002, India. <sup>3</sup>Biotechnology Group, Biological Sciences & Technology Division (BSTD), CSIR-North East Institute of Science & Technology, Jorhat 785006, Assam, India. ✉email: spsaikia@gmail.com

|                                      | <i>ITS2</i> | <i>matK</i> | <i>rbcl</i> | <i>ycf1</i> | <i>ITS2 + matK</i> | <i>ITS2 + rbcl</i> | <i>ITS2 + ycf1</i> | <i>matK + rbcl</i> | <i>matK + ycf1</i> | <i>rbcl + ycf1</i> | <i>ITS2 + matK + rbcl</i> | <i>ITS2 + matK + ycf1</i> | <i>ITS2 + rbcl + ycf1</i> | <i>matK + rbcl + ycf1</i> | <i>ITS2 + matK + rbcl + ycf1</i> |
|--------------------------------------|-------------|-------------|-------------|-------------|--------------------|--------------------|--------------------|--------------------|--------------------|--------------------|---------------------------|---------------------------|---------------------------|---------------------------|----------------------------------|
| No. of species samples (individuals) | 118 (13)    | 106 (12)    | 119 (16)    | 89 (9)      | 102 (11)           | 97 (11)            | 88 (9)             | 97 (12)            | 87 (9)             | 82 (9)             | 93 (11)                   | 86 (9)                    | 82 (9)                    | 82 (9)                    | 80 (9)                           |
| PCR success (%)                      | 100         | 100         | 100         | 100         | –                  | –                  | –                  | –                  | –                  | –                  | –                         | –                         | –                         | –                         | –                                |
| Sequencing success (%)               | 93.6        | 95.7        | 90.4        | 94.6        | –                  | –                  | –                  | –                  | –                  | –                  | –                         | –                         | –                         | –                         | –                                |
| Aligned sequenced length (bp)        | 307         | 759         | 516         | 872         | 1,067              | 837                | 1,193              | 1,275              | 1,631              | 1,388              | 1,583                     | 1,939                     | 1,696                     | 2,147                     | 2,455                            |
| No. of variable sites                | 98          | 103         | 20          | 59          | 264                | 115                | 139                | 125                | 158                | 78                 | 219                       | 246                       | 162                       | 177                       | 164                              |
| No. of parsimony informative sites   | 75          | 100         | 18          | 52          | 244                | 104                | 131                | 119                | 151                | 75                 | 205                       | 228                       | 149                       | 169                       | 144                              |
| Indel length                         | 3           | 3           | 0           | 2           | 15                 | 11                 | 5                  | 6                  | 7                  | 3                  | 14                        | 18                        | 13                        | 8                         | 20                               |
| No. of conserved sites               | 209         | 656         | 496         | 813         | 865                | 708                | 1,040              | 1,150              | 1,473              | 1,310              | 1,363                     | 1,692                     | 1,533                     | 1,970                     | 2,190                            |

**Table 1.** Assessment of four barcodes and its combinations:

that were not practicable for data input. To resolve the issue, we attempted to develop two dimensional QR code by encoding the DNA sequences of *Clerodendrum*, which could further help any non-taxonomist to easily recognize the species in the field through direct scanning of DNA QR code label via mobile devices. Further, this study could lead to valuable aid in the conservation of biodiversity strategies and the improvement of the genus.

## Results:

**Amplification and sequencing success.** The efficient PCR amplification and sequencing were regarded as a critical indicator for evaluating the barcode candidates. In this study, the success rate of PCR amplification for four loci (*ITS2*, *matK*, *rbcl* and *ycf1*) were 100% and sequencing rates were maximum for *matK* (95.7%) followed by *ycf1* (94.6%), *ITS2* (93.6%) and *rbcl* (90.4%) respectively (Table 1). A total of 352 new sequences from 9 *Clerodendrum* sp. were submitted to NCBI that includes 88, 90, 85, and 89 sequences of *ITS2*, *matK*, *rbcl*, and *ycf1*. The submitted sequences were analysed together with retrieved sequences of NCBI and attained a sum of 432 sequences that consist of 118, 106, 119, and 89 sequences of *ITS2*, *matK*, *rbcl*, and *ycf1*.

**Characteristic analysis of each barcode locus.** The ambiguous terminal sequences were deleted from the aligned sequence. The length of aligned sequences for each locus and combination of locus were ranged from 307 bp of *ITS2* to 2455 bp of *ITS2 + matK + rbcl + ycf1*. Among the single locus, *matK* had the maximum variable and parsimony-informative characters followed by *ITS2*. *ITS2 + matK* had maximum variability and parsimony informative sites (264/244) among the combinational locus (Table 1). In this study, the mean inter-specific distances were much higher than intra-specific distances. The pairwise intra-specific distances among the fifteen barcodes ranged from 0.0 to  $0.044 \pm 0.004$  and the mean intra-specific distances was maximum for *matK* ( $0.021 \pm 0.001$ ) and least for *rbcl + ycf1* ( $0.001 \pm 0.000$ ). Subsequently, the pairwise inter-specific distances were ranged from 0.0 to  $0.151 \pm 0.005$  and the mean inter-specific distances was highest for *matK* ( $0.086 \pm 0.005$ ) and least for *matK + rbcl* ( $0.011 \pm 0.003$ ) (Table 2). In precise, *matK* reveal the highest mean intra- and inter-specific distances.

**DNA barcode gap analysis.** Fundamentally, an ideal barcode should show significant “barcode gap” that defined the spacer region between the range of inter and intra-specific divergences<sup>12</sup>. The existence of barcode gap were evaluated at a class interval of 0.005 distance units between inter and intra-specific divergences. Among the fifteen barcodes, significant barcode gap was observed in the plastid gene *matK*, nucleotide locus *ITS2* and *ITS2 + matK* with the least overlap values, whereas the other genes revealed the unclear gaps with overlapped of intra- and inter-specific distances (Fig. 1).

**Species discrimination.** For discriminating species using TaxonDNA, *ITS2 + matK* had the highest success rate for correct identification of species (Best match: 96.11%; Best close match: 96.11%; All species barcodes: 84.50%) followed by *matK*, *ITS2*, *ITS2 + matK + ycf1*, and *rbcl + ycf1* had the lowest discriminatory rate (Best match: 36.34%; Best close match: 36.34%; All species barcodes: 28.78%) (Table 3).

**Phylogenetic analyses.** The barcode loci were analysed with BI, ML and NJ phylogenetic trees and generated similar discriminatory results with reliable clade support. The PP (Posterior Probability) values based on BI tree were higher than the bootstraps values of ML and NJ trees. The rate of discriminatory success for single and multi-locus barcodes were estimated based on percentage of species resolution for each species and determined to be monophyletic. Both the single and multi-locus barcodes showed different levels of species discrimination varying from 33.3 to 93.2% (Table 4). Amongst the single locus, *matK* (BI-91.6, ML-91.6, NJ-91.6) followed by *ITS2* (BI-84.6, ML-84.6, NJ-84.6) showed relatively high levels of discriminating success rates, whereas *rbcl* (BI-60.2, ML-55.2, NJ-59.6) had lowest level of discriminations. Combination of both *ITS2* and *matK* resolved maximum success rate of discrimination (BI-93.2, ML-91.9, NJ-93.2) as compared with other combinatorial loci

| Barcode locus                    | Intraspecific distances (%) |                   |                   | Interspecific distances (%) |                   |                   |
|----------------------------------|-----------------------------|-------------------|-------------------|-----------------------------|-------------------|-------------------|
|                                  | Minimum                     | Maximum $\pm$ S.D | Mean $\pm$ S.D    | Minimum                     | Maximum $\pm$ S.D | Mean $\pm$ S.D    |
| <i>ITS2</i>                      | 0                           | 0.029 $\pm$ 0.019 | 0.016 $\pm$ 0.005 | 0                           | 0.100 $\pm$ 0.023 | 0.044 $\pm$ 0.006 |
| <i>matK</i>                      | 0                           | 0.044 $\pm$ 0.004 | 0.021 $\pm$ 0.001 | 0                           | 0.151 $\pm$ 0.005 | 0.086 $\pm$ 0.005 |
| <i>rbcL</i>                      | 0                           | 0.015 $\pm$ 0.005 | 0.008 $\pm$ 0.001 | 0                           | 0.025 $\pm$ 0.006 | 0.019 $\pm$ 0.004 |
| <i>ycf1</i>                      | 0                           | 0.018 $\pm$ 0.004 | 0.011 $\pm$ 0.001 | 0                           | 0.032 $\pm$ 0.005 | 0.026 $\pm$ 0.004 |
| <i>ITS2 + matK</i>               | 0                           | 0.036 $\pm$ 0.006 | 0.013 $\pm$ 0.002 | 0                           | 0.109 $\pm$ 0.010 | 0.040 $\pm$ 0.006 |
| <i>ITS2 + rbcL</i>               | 0                           | 0.041 $\pm$ 0.007 | 0.007 $\pm$ 0.001 | 0                           | 0.059 $\pm$ 0.008 | 0.027 $\pm$ 0.006 |
| <i>ITS2 + ycf1</i>               | 0                           | 0.037 $\pm$ 0.005 | 0.010 $\pm$ 0.002 | 0                           | 0.058 $\pm$ 0.007 | 0.030 $\pm$ 0.005 |
| <i>matK + rbcL</i>               | 0                           | 0.013 $\pm$ 0.002 | 0.002 $\pm$ 0.001 | 0                           | 0.064 $\pm$ 0.007 | 0.011 $\pm$ 0.003 |
| <i>matK + ycf1</i>               | 0                           | 0.015 $\pm$ 0.003 | 0.003 $\pm$ 0.001 | 0                           | 0.057 $\pm$ 0.006 | 0.021 $\pm$ 0.003 |
| <i>rbcL + ycf1</i>               | 0                           | 0.013 $\pm$ 0.003 | 0.001 $\pm$ 0.000 | 0                           | 0.025 $\pm$ 0.004 | 0.015 $\pm$ 0.003 |
| <i>ITS2 + matK + rbcL</i>        | 0                           | 0.026 $\pm$ 0.004 | 0.006 $\pm$ 0.001 | 0                           | 0.073 $\pm$ 0.007 | 0.018 $\pm$ 0.004 |
| <i>ITS2 + matK + ycf1</i>        | 0                           | 0.027 $\pm$ 0.003 | 0.009 $\pm$ 0.001 | 0                           | 0.067 $\pm$ 0.005 | 0.033 $\pm$ 0.003 |
| <i>ITS2 + rbcL + ycf1</i>        | 0                           | 0.028 $\pm$ 0.003 | 0.006 $\pm$ 0.001 | 0                           | 0.045 $\pm$ 0.005 | 0.022 $\pm$ 0.003 |
| <i>matK + rbcL + ycf1</i>        | 0                           | 0.013 $\pm$ 0.002 | 0.003 $\pm$ 0.001 | 0                           | 0.046 $\pm$ 0.004 | 0.017 $\pm$ 0.002 |
| <i>ITS2 + matK + rbcL + ycf1</i> | 0                           | 0.022 $\pm$ 0.003 | 0.005 $\pm$ 0.001 | 0                           | 0.054 $\pm$ 0.004 | 0.025 $\pm$ 0.003 |

**Table 2.** Summary of the pairwise intra-specific and inter-specific distances in *Clerodendrum* genus. S.D standard deviation.

of barcodes. Hence, it could be concluded that species discrimination was high when *matK* was included among other combinations.

The phylogenetic tree of *ITS2 + matK* was reconstructed with BI method and nodal support value of ML and NJ as depicted in Fig. 2. In the phylogenetic tree, *Clerodendrum* species were well separated from outgroup and considered to be monophyletic. The phylogenetic tree was divided into 9 clades with moderate to high bootstraps and PP supports values. The Clade 1 consists of *C. colebrookianum* with 0.71 of BI support and 100% of ML and NJ bootstrap. In Clades 3, 4, 6, 7, 8, and 9 form clear individual clusters for species of *C. infortunatum*, *C. indicum*, *C. thomsoniae*, *C. philipinum*, *C. inerme*, and *C. serratum*. The species of *C. cryptophyllum* and *C. canescent* in Clade 2 (BI-1.00, ML-73%, NJ-89%) and *C. japonicum* and *C. paniculatum* in Clade 5 (BI-1.00, ML-100%, NJ-100%) were grouped together in each clade which signified that they were closely related.

Thus, we tentatively proposed *ITS2 + matK* gene with significant barcode gap and strong discriminatory power could be the preeminent barcode for *Clerodendrum* species.

**Two-Dimensional DNA barcode generation.** At present, “DNA barcode” refers to the DNA sequences which were inadequate for storing data, recognition, and information retrieval. This could be resolved with the two-dimensional QR codes that could represent DNA barcode sequences efficiently. The *ITS2 + matK* barcode marker of *Clerodendrum* species were transformed into QR codes with a motive to benefit the diverse researchers with no prior knowledge of DNA barcoding (Fig. 3).

## Discussion

An efficient barcode should be easily amplified, sequenced and resolve with high species discrimination and identification<sup>13,14</sup>. The four barcode markers used in this study were the universal plant markers with suitable length and cost effective<sup>15</sup>. In the present study, we analysed both the sequences of *Clerodendrum* sp. and repository sequences of GenBank records. Among the four-barcode locus, *matK* and *ycf1* produces high quality of sequences as compared to *ITS2* and *rbcL*. Among the markers, *matK* performed the best with high species resolutions and clear barcoding gaps followed by *ITS2*. The efficacy of *matK* was also supported in previous researches as core barcode for many plants genera due to its high amount of variability and results in a high rate of molecular evolution as compared to the other barcode coding regions<sup>16,17</sup>. Moreover, *ITS2* was considered as a complementary marker to the core barcodes<sup>18,19</sup> and many studies had reported its high rate of variability in discriminating the species<sup>20,21</sup>. Many researchers proposed *ITS2* as a standard marker for identification of more than 6,600 plant specimens from 753 genera and universal barcode for medicinal plant species<sup>22,23</sup>.

The plastid gene *ycf1* was recently proposed as an effective barcode marker in angiosperms due to its high amount of variability<sup>24</sup>. This gene was reported to be a probable phylogenetic marker for plants like pines, orchid, etc.<sup>25</sup>. Simultaneously, the chloroplast coding region *rbcL* was proposed as a universal primer for ferns, mosses, and angiosperms<sup>7,26</sup>. But in some recent studies, *rbcL* was reported to be incongruous barcode marker due to its low inter-specific variations even in closely related species<sup>20,27</sup>. Conversely, in this study both the markers restrained the lowest number of variation site, parsimony informative sites and species discriminating rates. The complexities of these chloroplast markers prevent discrimination of species, as it represents only the maternal inheritance variation<sup>28</sup>. Thus, it could be suggested that *ycf1* and *rbcL* region were not suitable for DNA barcoding in *Clerodendrum* species.

Several combinations of two, three and four barcodes were analysed in this study. The combination of *matK + rbcL* was proposed to be the universal barcode for all the land plants by CBOL in 2009, but in this study,

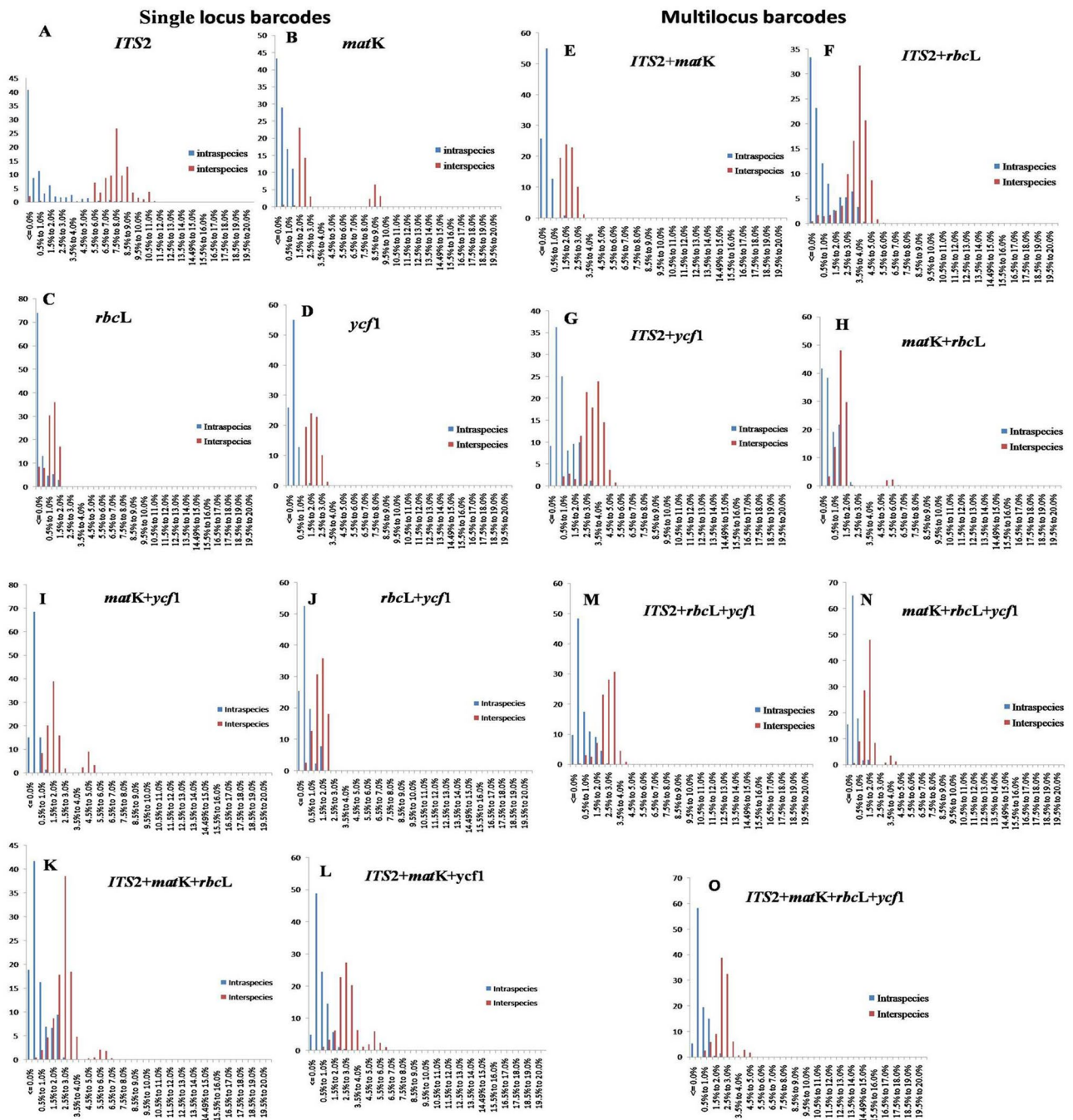


**Figure 1.** Distribution of intra- and inter-specific Kimura 2-parameter (K2P) distances among all *Clerodendrum* samples for the four barcodes loci and their combinations.

it possesses lowest species resolutions among all the combinatorial barcode markers due to its low substitution rates. In contrast, the combination of *ITS2 + matK* represents the highest percentage of species resolution with clear barcode gaps as compared to both single and combination of markers and also relate similarities with the previous findings<sup>29,30</sup>.

The barcoding gap that exists between the highest intra-specific value and the lowest inter-specific value could depict the limits of species variation within a genus and a threshold limit of species can be set<sup>31,32</sup>. Overlaps of the threshold value signify cryptic species and probably show insignificant variation with the barcode. Among the single and multi-locus barcode, *matK* and *ITS2 + matK* possess clear barcode gap compared to the other barcode markers. The statistics of best match, best close match and all species barcodes using TaxonDNA was used to evaluate the rate of species identification<sup>9,33</sup> and observed that *ITS2 + matK* followed by *matK* possess high rate of species discriminations. Based on phylogenetic tree methods, *ITS2 + matK* specifies maximum rate of species resolution in *Clerodendrum*. Similar levels of resolvability by different tree-methods were reported in Lamiaceae<sup>34</sup>.

| Regions                          | Best match  |               |               | Best close match |               |               | All species barcodes |               |               | Threshold Value |
|----------------------------------|-------------|---------------|---------------|------------------|---------------|---------------|----------------------|---------------|---------------|-----------------|
|                                  | Correct (%) | Ambiguous (%) | Incorrect (%) | Correct (%)      | Ambiguous (%) | Incorrect (%) | Correct (%)          | Ambiguous (%) | Incorrect (%) |                 |
| <i>ITS2</i>                      | 91.34       | 1.21          | 2.43          | 91.34            | 12.47         | 2.96          | 79.79                | 17.96         | 0.0           | 1.92            |
| <i>matK</i>                      | 94.56       | 3.77          | 5.66          | 94.12            | 6.56          | 1.66          | 74.9                 | 35.09         | 0.0           | 1.30            |
| <i>rbcL</i>                      | 48.48       | 28.15         | 3.36          | 48.48            | 28.15         | 3.36          | 31.09                | 67.22         | 1.68          | 1.35            |
| <i>ycf1</i>                      | 87.64       | 7.86          | 4.49          | 81.64            | 7.86          | 3.37          | 62.92                | 37.07         | 0.0           | 1.02            |
| <i>ITS2 + matK</i>               | 96.11       | 3.96          | 1.92          | 96.11            | 7.96          | 3.92          | 84.50                | 15.48         | 0.0           | 2.80            |
| <i>ITS2 + rbcL</i>               | 75.25       | 12.37         | 2.37          | 75.25            | 0.0           | 11.25         | 20.61                | 79.38         | 0.0           | 3.30            |
| <i>ITS2 + ycf1</i>               | 62.04       | 1.13          | 6.81          | 62.04            | 7.13          | 6.81          | 59.54                | 70.45         | 0.0           | 2.27            |
| <i>matK + rbcL</i>               | 50.72       | 6.18          | 3.09          | 50.32            | 5.06          | 3.09          | 42.26                | 57.73         | 0.0           | 0.86            |
| <i>matK + ycf1</i>               | 82.69       | 10.0          | 0.0           | 82.65            | 0.0           | 0.0           | 48.16                | 20.68         | 0.0           | 0.73            |
| <i>rbcL + ycf1</i>               | 36.34       | 1.21          | 2.43          | 36.34            | 3.63          | 2.43          | 28.78                | 50.0          | 1.21          | 0.86            |
| <i>ITS2 + matK + rbcL</i>        | 65.69       | 1.07          | 3.22          | 62.04            | 11.07         | 3.22          | 24.73                | 75.26         | 0.0           | 2.01            |
| <i>ITS2 + matK + ycf1</i>        | 90.34       | 0.0           | 4.65          | 90.34            | 0.0           | 4.65          | 55.81                | 44.18         | 0.0           | 1.64            |
| <i>ITS2 + rbcL + ycf1</i>        | 51.46       | 0.0           | 1.53          | 51.37            | 0.0           | 8.53          | 25.6                 | 74.39         | 0.0           | 1.95            |
| <i>matK + rbcL + ycf1</i>        | 60.28       | 0.0           | 0.0           | 60.28            | 0.0           | 0.0           | 45.85                | 32.94         | 0.0           | 0.64            |
| <i>ITS2 + matK + rbcL + ycf1</i> | 76.25       | 0.0           | 3.75          | 61.55            | 0.0           | 19.75         | 37.5                 | 62.5          | 0.0           | 1.14            |

**Table 3.** Species identification based on the ‘best match’, ‘best close match’ and ‘all species barcodes’ with TaxonDNA software.

| Regions                          | Species resolution (%) |      |      |
|----------------------------------|------------------------|------|------|
|                                  | BI                     | ML   | NJ   |
| <i>ITS2</i>                      | 84.6                   | 84.6 | 84.6 |
| <i>matK</i>                      | 91.6                   | 91.6 | 91.6 |
| <i>rbcL</i>                      | 60.2                   | 55.2 | 59.6 |
| <i>ycf1</i>                      | 77.7                   | 60.3 | 72.4 |
| <i>ITS2 + matK</i>               | 93.2                   | 91.9 | 93.2 |
| <i>ITS2 + rbcL</i>               | 63.6                   | 52.6 | 54.5 |
| <i>ITS2 + ycf1</i>               | 77.7                   | 64.1 | 77.7 |
| <i>matK + rbcL</i>               | 59.7                   | 58.3 | 59.7 |
| <i>matK + ycf1</i>               | 78.8                   | 77.7 | 78.8 |
| <i>rbcL + ycf1</i>               | 35.1                   | 33.3 | 35.1 |
| <i>ITS2 + matK + rbcL</i>        | 72.7                   | 63.6 | 72.7 |
| <i>ITS2 + matK + ycf1</i>        | 88.8                   | 77.7 | 88.8 |
| <i>ITS2 + rbcL + ycf1</i>        | 77.7                   | 77.7 | 77.7 |
| <i>matK + rbcL + ycf1</i>        | 66.6                   | 55.5 | 66.6 |
| <i>ITS2 + matK + rbcL + ycf1</i> | 88.8                   | 88.8 | 88.8 |

**Table 4.** Species discrimination rate of all barcodes loci in *Clerodendrum* species.

In recent trends, DNA barcode encounters limitation in its practical applications due to the lack of information compression and retrieval of information through direct scanning of DNA sequences<sup>35</sup>. Therefore, an easy innovative format and rapid retrieving barcode information is in need. Barcode technology was well established in manufacturing and retailing industries for a couple of decades. The QR code contains meaningful information in both vertical and horizontal direction more than the data carried by vertical lines of barcodes (stores maximum of 20 digits). This technique could detect symbols that lead to a specific product. If this technology was applied to represent the sequences of DNA barcodes then it could lead to efficient retrieval of information with the largest coding capacity and high compression ratio, as reported by Liu et al. In this study, *ITS2 + matK* barcode sequences for 9 *Clerodendrum* sp. were converted to QR codes with vivid sequence information. The QR code could monitor the different species of *Clerodendrum* from its origin even in the field; ensure the mislabeling and safety of its commercial product.

Hence, the barcode marker *ITS2 + matK* could be used as superlative locus to determine the species boundary in *Clerodendrum*. Optimization of these results for all the species of *Clerodendrum* was not advisable as this study was constraint to North East region of India but this could lay the foundation for the universal use of DNA barcoding in plants. The success rate of species identification would be more confirmed if more species were included further<sup>36</sup>. Therefore, a potential solution for identifying species based on geographical location and sampling size should be further investigated. In the upcoming years, these findings would be potentially helpful in delineating the large genus of *Clerodendrum*.

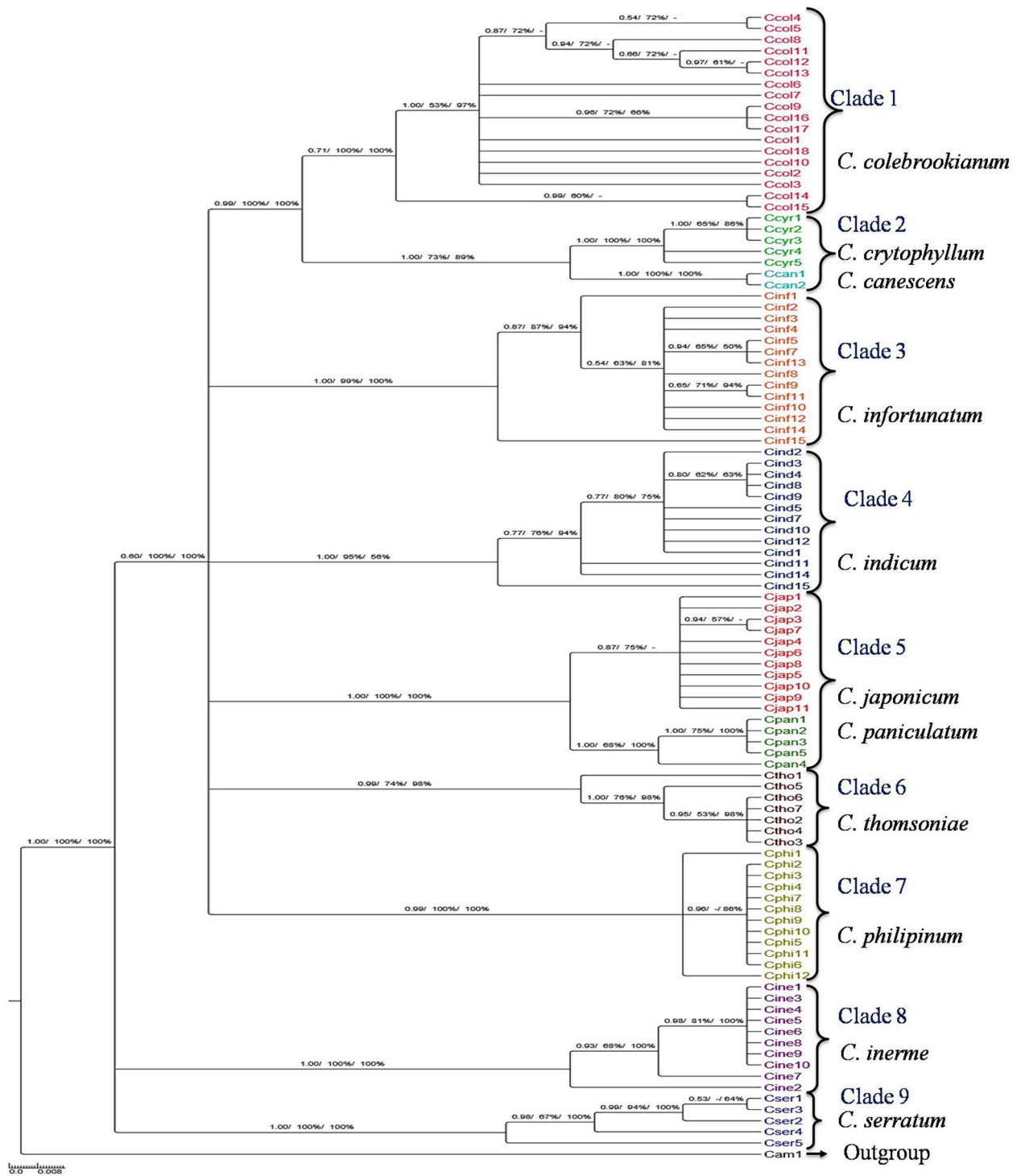


**Figure 2.** Phylogenetic BI tree inferred from ITS2 + *matK* region of *Clerodendrum* sp. Result for ML and NJ bootstrap analysis were mapped onto BI tree. The node number indicates BI/ML/NJ values. BI with PP > 0.5, ML and NJ with bootstrap > 50% were shown. The scale bar corresponds to 0.8 substitutions per 100 nucleotide positions.

### Methods

**Sample collection and genomic DNA extraction.** A total of 94 samples from 9 species of *Clerodendrum* were collected from different locations of North East India. The numbers of collected samples for each species of *Clerodendrum* were depicted in Fig. 4. Tender leaf samples were collected and lyophilized at  $-110^{\circ}\text{C}$  for 48 h. Genomic DNA for the collected samples were extracted using modified CTAB method<sup>37</sup>. The quantity and quality of the extracted DNA were evaluated in Bio-spectrophotometer (Eppendorf, Germany), analysed in 0.8% agarose gel electrophoresis and visualized in gel documented system (G:BOX, Syngene, U.K.).

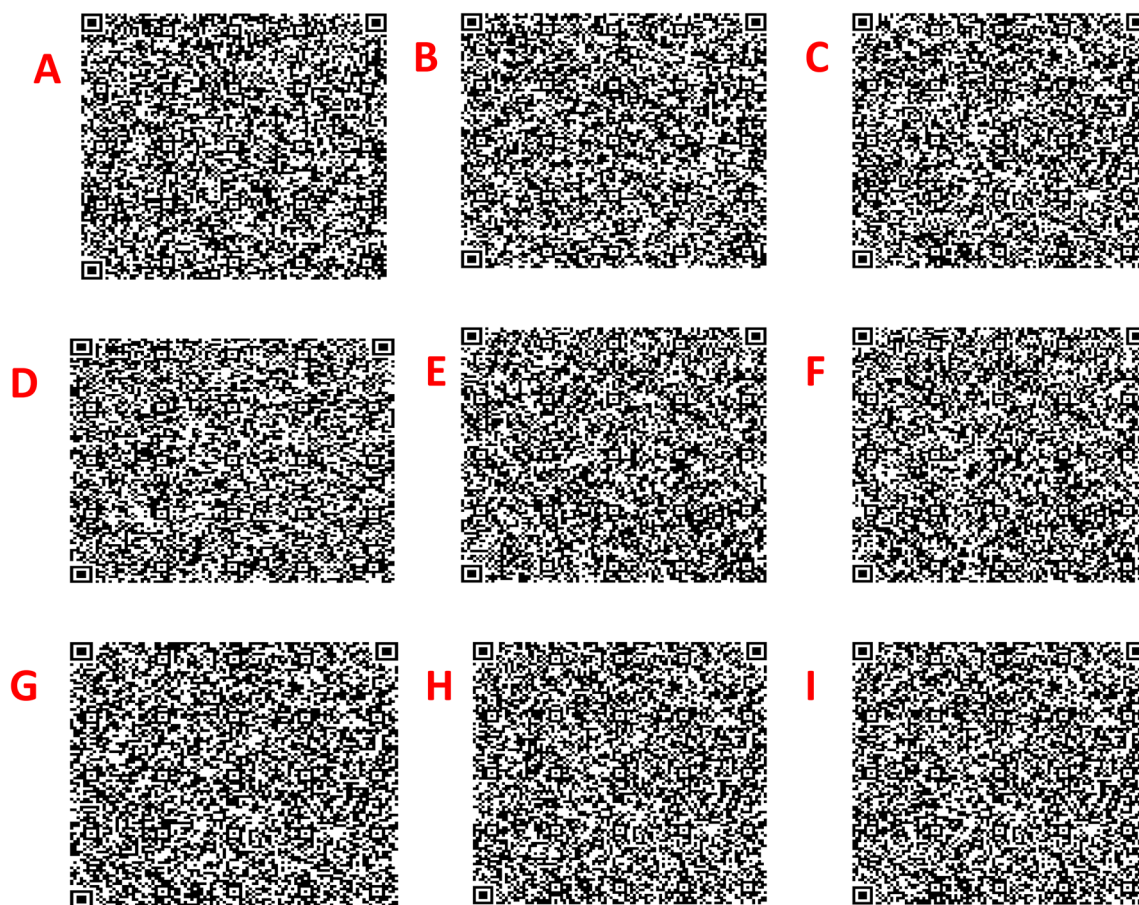


**Figure 3.** DNA sequence based QR code for species represented as (A) *C. colebrookianum*, (B) *C. infortunatum*, (C) *C. philippinum*, (D) *C. inerme*, (E) *C. indicum*, (F) *C. serratum*, (G) *C. thomsoniae*, (H) *C. paniculatum*, (I) *C. japonicum*.

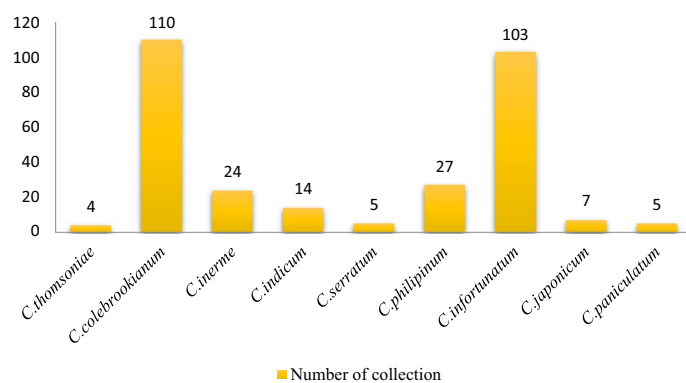


**Figure 4.** Graphical representation of collected *Clerodendrum* samples.

**PCR amplification, sequencing and sequence download.** The extracted DNA samples were amplified with *ITS2*, *matK*, *rbcl*, and *ycf1* in polymerase chain reaction (PCR) system (Applied Biosystem). The PCR mixtures (20ul each) contained 10 ng of template DNA, 10X PCR buffer with 1.5 mM of MgCl<sub>2</sub>, 2.5 mM dNTP, 1 unit/uL Taq DNA polymerase, 5 pmol of each primer and adjusted the final volume with nuclease free ddH<sub>2</sub>O. The PCR conditions for each selected barcode primer were listed in (Table 5). For bidirectional sequencing, the amplified products were sent to Eurofins Genomics India Private Limited Company using the same primers to resolve ambiguities.

Additionally, we retrieved all the sequences (*ITS2*, *matK*, *rbcl* and *ycf1*) of *Clerodendrum* from NCBI database. The downloaded sequences were filtered based on the criteria that: (i) sequence length less than 300 bp and (ii) sequences lacking specific voucher names. According to our survey, some species contain less than five sequences

| Regions | Primer | Sequence (5'–3')             | PCR conditions  | References |
|---------|--------|------------------------------|---|------------|
| ITS2    | ITS2 F | ATGCGATACTTGGTGTGAAT         | 94 °C-4 min, (94 °C-30 s, 53 °C-40 s, 72 °C-40 s) 40 cycles and final extension with 72 °C-7 min    | 51         |
|         | ITS2 R | GACGCTTCTCCAGACTACAAT        |   |            |
| matK    | 3FKIM  | CGTACAGTACTTTTGTGTTTACGAG    | 95 °C-4 min, (95 °C-30 s, 50 °C-40 s, 72 °C-50 s) 35 cycles and final extension with 72 °C-2 min    | 52         |
|         | 1RKIM  | ACCCAGTCCATCTGGAAATCTTGGTTC  |   |            |
| rbcL    | aF     | ATGTCACCACAAACAGAGACTAAAGC   | 94 °C-7 min, (94 °C-1 min, 51 °C-30 s, 72 °C-1 min) 35 cycles and final extension with 72 °C-10 min | 53         |
|         | aR     | GTAATAATCAAGTCCACCRGC        |   |            |
| ycf1    | F      | TCTCGACGAAAATCAGATTGTTGTGAAT | 94 °C-4 min, (94 °C-30 s, 52 °C-40 s, 72 °C-1 min) 35 cycles and final extension with 72 °C-10 min  | 24         |
|         | R      | ATACATGTCAAAGTGATGGAAA       |   |            |

**Table 5.** Details of primer used in the study.

in NCBI while some species had maximum number of sequences for a specific barcode region. Therefore, the representatives for each species were restricted between five to eighteen samples. The taxa, voucher names and accession number used in this study were provided in (Table S1).

**Data analysis.** The sequences of each barcode were aligned with MUSCLE (<https://www.ebi.ac.uk/Tools/msa/muscle>) and edited manually in BioEdit v7.1.3.0<sup>38</sup>. For ITS2 region, the sequences were subjected to Hidden Markov Model (HMM) to remove the conserved 5.8S and 28S DNA sequences<sup>39</sup>. The edited sequences were compared with available nucleotide sequences of GenBank database and submitted to NCBI and BOLD databases with project code-NECLE (Table S2). The analyses of genetic pairwise distances were computed in MEGA X<sup>40</sup> with Kimura-2-parameter (K2P) model. The K2P was considered as the most favourable model for small distance calculations<sup>41</sup>. Differences between intra- and inter-specific distances with four single barcodes were evaluated using pairwise distance matrix in MEGA X software. An ideal barcode could be determined with the presence of barcoding gap, that compared the intra- and inter-specific distance distribution for each barcode candidate with an interval distance of 0.05 in TaxonDNA with 'pairwise summary function'<sup>42</sup>. In TaxonDNA, best match, best close match, and all species barcodes functions were intended to examine the accurate identification proportion of each barcode. The 'Best match' analyses determine the closest adjoining match for a known sequence. If the examined sequences were from the analogous species then the identification was considered correct whereas incorrect if the sequences belong to different species<sup>29</sup>.

**Phylogenetic analysis.** The species discriminatory efficacy of each single and multi-locus barcode candidates was assessed with three tree-based method, which include the Neighbour-joining (NJ) tree, Maximum likelihood (ML) tree and Bayesian inference (BI) tree. The NJ methods of all markers were conducted using MEGA X<sup>43,44</sup>. The reliability of node was supported by bootstrap test of 1,000 pseudo-replicates with K2P distance parameter. For ML analysis, the phylogenetic trees were constructed in RAXMLGUI v1.3.1, a graphical front-end for RAXML<sup>45</sup>. The clade support was assessed using ML with thorough bootstrap analyses, run 10 times starting from random seeds under GTRGAMMA model and 1,000 non-parametric bootstrap values<sup>46</sup>. The species forming separate clusters in the tree with bootstrap support > 50% were considered to be distinct. The analysis of BI trees was conducted in MrBayes v3.2.7<sup>47</sup>. The best substitution models of each locus were selected according to Akaike information criterion (AIC) with jModeltest version 2.1.7<sup>48</sup>. The model suggested by jModeltest was GTR + I + G for all the tested barcode except GTR + G model for *matK*. The two replicate runs of Markov chain Monte Carlo (MCMC) were run for 5,000,000 generations with four simultaneous chains (one cold and three hot chains), and trees were sampled at every 1000th generations. The adequate posterior probability (PP) distribution of samples were determined, when the split frequency of average standard deviation was lower than 0.01. Subsequently, the stationary was determined in Tracer v1.7.1<sup>49</sup> and the first 25% trees were discarded as burn-in and a 50% majority-rule consensus tree was constructed and PP was considered as node support values. All the topologies of trees were visualized in FigTree v1.4.4. Percentages of species resolutions were calculated from the reconstructed tree in order to resolve the monophyletic nature of the clades. *Callicarpa americanaw* was used as an outgroup.

**Generation of QR code.** The two-dimensional QR code consists of black modules with three squares on the corner of the code on white background and could involve 7,089 numeric, 4,296 alphanumeric characters, and 2,953 bytes of binary data<sup>50</sup>. In this study, the QR code image for the candidate barcode marker was generated by DNA QR Code Web Server<sup>35</sup>.

### Data availability

We retrieved GenBank accessions of *ITS2*, *matK*, *rbcL* and *ycf1* for *Clerodendrum* sp. and details are included in Table S1 (Supporting Information). Submitted sequences of *Clerodendrum* species were included in Table S2.

Received: 4 March 2020; Accepted: 6 July 2020

Published online: 10 August 2020

## References

1. Wahba, H. M. *et al.* Chemical and biological investigation of some *Clerodendrum* species cultivated in Egypt. *Pharm. Biol.* **49**(1), 66–72 (2011).
2. Leeratiwong, C., Chantaranonthai, P. & Paton, A. J. A synopsis of the genus *Clerodendrum* L. (Lamiaceae) in Thailand. *Trop. Nat. Hist.* **11**(2), 177–211 (2011).
3. Deori, C., Roy, D. K., Talukdar, S. R., Pagag, K. & Sarma, N. Diversity of the genus *Clerodendrum* Linnaeus (Lamiaceae) in Northeast India with special reference to Barnadi Wildlife Sanctuary, Assam. *Pleione* **7**(2), 473–488 (2013).
4. Yuan, Y. W. *et al.* Further disintegration and redefinition of *Clerodendrum* (Lamiaceae): implications for the understanding of the evolution of an intriguing breeding strategy. *Taxon* **59**, 125–133 (2010).
5. Steane, D. A. *et al.* Phylogenetic relationships between *Clerodendrum* (Lamiaceae) and other Ajugoid genera inferred from nuclear and chloroplast DNA sequence data. *Mol. Phylogenet. Evol.* **32**, 39–45 (2004).
6. Shrivastava, N. & Patel, T. *Clerodendrum* and healthcare: an overview. *Med. Aromat. Plant. Sci. Biotechnol.* **1**(1), 142–150 (2007).
7. Chase, M. W. *et al.* A proposal for a standardised protocol to barcode all land plants. *Taxon* **56**(2), 295–299 (2007).
8. Singh, H. K., Parveen, I., Raghuvanshi, S. & Babbar, S. B. The loci recommended as universal barcodes for plants on the basis of floristic studies may not work with congeneric species as exemplified by DNA barcoding of *Dendrobium* species. *BMC research notes* **5**(1), 42 (2012).
9. Giudicelli, G., Mader, G. & Brandao de Freitas, L. Efficiency of ITS sequences for DNA barcoding in *Passiflora* (Passifloraceae). *Int. J. Mol. Sci.* **16**(4), 7289–7303 (2015).
10. Kane, N. *et al.* Ultra-barcoding in cacao (*Theobroma* spp.; Malvaceae) using whole chloroplast genomes and nuclear ribosomal DNA. *Am. J. Bot.* **99**(2), 320–329 (2012).
11. Yu, N. *et al.* Barcode ITS2: a useful tool for identifying *Trachelospermum jasminoides* and a good monitor for medicine market. *Sci. Rep.* **7**(1), 5037 (2017).
12. Meyer, C. P. & Paulay, G. DNA barcoding: error rates based on comprehensive sampling. *PLoS Biol.* **3**(12), e422 (2005).
13. Hollingsworth, P. M., Graham, S. W. & Little, D. P. Choosing and using a plant DNA barcode. *PLoS ONE* **6**(5), e19254 (2011).
14. Yang, J. B., Wang, Y. P., Moeller, M., Gao, L. M. & Wu, D. Applying plant DNA barcodes to identify species of *Parnassia* (Parnassiaceae). *Mol. Ecol. Resour.* **12**(2), 267–275 (2012).
15. Kress, W. J. Plant DNA barcodes: applications today and in the future. *J. Syst. Evol.* **55**, 291–307 (2017).
16. Parveen, I., Singh, H. K., Raghuvanshi, S., Pradhan, U. C. & Babbar, S. B. DNA barcoding of endangered Indian *Paphiopedilum* species. *Mol. Ecol. Resour.* **12**(1), 82–90 (2012).
17. Chen, F. R., *et al.* Identification of *Chrysanthemum indicum* and its adulterants based on ITS2 barcode. *Zhongguo Zhongyao za zhi= Zhongguo zhongyao za zhi= China Journal of Chinese Materia Medica*, **44**(4), 654–659 (2019).
18. CBOL Group. A DNA barcode for land plants. *Proc. Natl. Acad. Sci. USA* **106**(31), 12794–12797 (2009).
19. Pawlowski, J. *et al.* CBOL protist working group: barcoding eukaryotic richness beyond the animal, plant, and fungal kingdoms. *PLoS Biol.* **10**(11), e1001419 (2012).
20. Kress, W. J., Wurdack, K. J., Zimmer, E. A., Weigt, L. A. & Janzen, D. H. Use of DNA barcodes to identify flowering plants. *Proc. Natl. Acad. Sci. USA* **102**(23), 8369–8374 (2005).
21. Sass, C., Little, D. P., Stevenson, D. W. & Specht, C. D. DNA barcoding in the cycadales: testing the potential of proposed barcoding markers for species identification of cycads. *PLoS ONE* **2**(11), e1154 (2007).
22. Pang, X., Song, J., Zhu, Y., Xie, C. & Chen, S. Using DNA barcoding to identify species within Euphorbiaceae. *Planta Med.* **76**(15), 1784–1786 (2010).
23. Han, J. *et al.* The short ITS2 sequence serves as an efficient taxonomic sequence tag in comparison with the full-length ITS. *BioMed Res. Int.* **2013**, 74146. <https://doi.org/10.1155/2013/741476> (2013).
24. Dong, W. *et al.* *ycf1*, the most promising plastid DNA barcode of land plants. *Sci. Rep.* **5**, 8348 (2015).
25. Thitikornpong, W., Palanuvej, C. & Ruangrunsi, N. DNA barcoding for authentication of the endangered plants in genus *Aquilaria*. *Thai J. Pharm. Sci.* **42**(4), 433–484 (2018).
26. Hollingsworth, M. L. *et al.* Selecting barcoding loci for plants: evaluation of seven candidate loci with species level sampling in three divergent groups of land plants. *Mol. Ecol. Resour.* **9**(2), 439–457 (2009).
27. Steven, G. N. & Subramanyam, R. Testing plant barcoding in a sister species complex of pantropical *Acacia* (Mimosoideae, Fabaceae). *Mol. Ecol. Resour.* **9**, 172–180 (2009).
28. Vu, T. H. T., Le, T. L., Nguyen, T. K., Tran, D. D. & Tran, H. D. Review on molecular markers for identification of orchids, Vietnam. *Int. J. Sci.* **59**(2), 62–75 (2017).
29. Xu, S. *et al.* Evaluation of the DNA barcodes in *Dendrobium* (Orchidaceae) from mainland Asia. *PLoS ONE* **10**(1), e0115168 (2015).
30. Cabelin, V. L. D. & Alejandro, G. J. D. Efficiency of *matK*, *rbcl*, *trnH-psbA*, and *trnL-F* (cpDNA) to molecularly authenticate Philippine ethnomedicinal Apocynaceae through DNA barcoding. *Pharmacogn. Mag.* **12**(3), S384 (2016).
31. Candek, K. & Kuntner, M. DNA barcoding gap: reliable species identification over morphological and geographical scales. *Mol. Ecol. Resour.* **15**(2), 268–277 (2015).
32. Chen, J., Zhao, J., Erickson, D. L., Xia, N. & Kress, W. J. Testing DNA barcodes in closely related species of *Curcuma* (Zingiberaceae) from Myanmar and China. *Mol. Ecol. Resour.* **15**(2), 337–348 (2015).
33. Krawczyk, K., Szczecinska, M. & Sawicki, J. Evaluation of 11 single locus and seven multilocus DNA barcodes in *Lamium* L. (Lamiaceae). *Mol. Ecol. Resour.* **14**(2), 272–285 (2014).
34. Theodoridis, S. *et al.* DNA barcoding in native plants of the Labiatae (Lamiaceae) family from Chios Island (Greece) and the adjacent Cesme-Karaburun Peninsula (Turkey). *Mol. Ecol. Resour.* **12**, 620–633 (2012).
35. Liu, C. *et al.* DNA barcode goes two-dimensions: DNA QR code web server. *PLoS ONE* **7**(5), e35146 (2012).
36. Kim, H. M., Oh, S. H., Bhandari, G. S., Kim, C. S. & Park, C. W. DNA barcoding of Orchidaceae in Korea. *Mol. Ecol. Resour.* **14**(3), 499–507 (2014).
37. Doyle, J. J. & Doyle, J. L. Isolation of plant DNA from fresh tissue. *Focus* **12**(13), 39–40 (1990).
38. Hall, T. A. BioEdit: a user-friendly biological sequence alignment editor and analysis program for Windows 95/98/NT. In *Nucleic Acids Symposium Series*, **41**, 95–98. [London]: Information Retrieval Ltd., c1979-c2000 (1999).
39. Gao, T. *et al.* Identification of medicinal plants in the family Fabaceae using a potential DNA barcode ITS2. *J. Ethnopharmacol.* **130**(1), 116–121 (2010).
40. Kumar, S., Stecher, G., Li, M., Knyaz, C. & Tamura, K. MEGA X: molecular evolutionary genetics analysis across computing platforms. *Mol. Biol. Evol.* **35**(6), 1547–1549 (2018).
41. Kimura, M. A simple method for estimating evolutionary rates of base substitutions through comparative studies of nucleotide sequences. *J. Mol. Evol.* **16**(2), 111–120 (1980).
42. Meier, R., Shiyang, K., Vaidya, G. & Ng, P. K. DNA barcoding and taxonomy in Diptera: a tale of high intraspecific variability and low identification success. *Syst. Biol.* **55**(5), 715–728 (2006).
43. Zhang, C. Y. *et al.* Testing DNA barcoding in closely related groups of *Lysimachia* L. (Myrsinaceae). *Mol. Ecol. Resour.* **12**(1), 98–108 (2012).
44. Alves, S. T. L., Chauveau, O., Eggers, L. & de Souza Chies, T. T. Species discrimination in *Sisyrinchium* (Iridaceae): Assessment of DNA barcodes in a taxonomically challenging genus. *Mol. Ecol. Resour.* **14**(2), 324–335 (2014).

45. Silvestro, D. & Michalak, I. RaxmlGUI: a graphical front-end for RAxML. *Org. Divers. Evol.* **12**(4), 335–337 (2012).
46. Zhang, H., Zhang, Y. & Duan, Y. DNA barcoding of *Deltocephalus Burmeister* leafhoppers (*Cicadellidae*, *Deltocephalinae*, *Deltocephalini*) in China. *ZooKeys.* **867**, 55 (2019).
47. Ronquist, F. *et al.* MRBAYES 3.2: Efficient Bayesian phylogenetic inference and model selection across a large model space. *Syst. Biol.* **61**, 539–542 (2012).
48. Li, Q. J. *et al.* Efficient identification of *Pulsatilla* (*Ranunculaceae*) using DNA barcodes and micro-morphological characters. *Front. Plant Sci.* **10**, 1196 (2019).
49. Rambaut, A., Drummond, A. J., Xie, D., Baele, G. & Suchard, M. A. Posterior summarization in Bayesian phylogenetics using Tracer 1.7. *Syst. Biol.* **67**(5), 901 (2018).
50. Naulia, T. DNA QR Code Scanner for Identifying the Species Origin of Meat Products. *ISICO 2015*, (2015).
51. Yao, H. *et al.* Use of *ITS2* region as the universal DNA barcode for plants and animals. *PLoS ONE* **5**(10), e13102 (2010).
52. Costion, C. *et al.* Plant DNA barcodes can accurately estimate species richness in poorly known floras. *PLoS ONE* **6**(11), e26841 (2011).
53. Maloukh, L. *et al.* Discriminatory power of *rbcl* barcode locus for authentication of some of United Arab Emirates (UAE) native plants. *3 Biotech.* **7**(2), 144 (2017).

## Acknowledgements

B.G. is thankful to Dr. G.N. Sastry, Director, CSIR-North East Institute of Science and Technology, Jorhat, Assam, India and Dr. S.P. Saikia and Dr. S.B. Wann for their consistent support in completing the manuscript. This study is financially supported by “CSIR-Direct SRF” fellowship under CSIR-HR Division, New Delhi.

## Author contributions

B.G. performed the experiment, analysed data and wrote the manuscript. S.P.S. designed the project and wrote the manuscript and S.B.W. provided technical support.

## Competing interests

The authors declare no competing interests.

## Additional information

**Supplementary information** is available for this paper at <https://doi.org/10.1038/s41598-020-70405-3>.

**Correspondence** and requests for materials should be addressed to S.P.S.

**Reprints and permissions information** is available at [www.nature.com/reprints](http://www.nature.com/reprints).

**Publisher’s note** Springer Nature remains neutral with regard to jurisdictional claims in published maps and institutional affiliations.



**Open Access** This article is licensed under a Creative Commons Attribution 4.0 International License, which permits use, sharing, adaptation, distribution and reproduction in any medium or format, as long as you give appropriate credit to the original author(s) and the source, provide a link to the Creative Commons license, and indicate if changes were made. The images or other third party material in this article are included in the article’s Creative Commons license, unless indicated otherwise in a credit line to the material. If material is not included in the article’s Creative Commons license and your intended use is not permitted by statutory regulation or exceeds the permitted use, you will need to obtain permission directly from the copyright holder. To view a copy of this license, visit <http://creativecommons.org/licenses/by/4.0/>.

© The Author(s) 2020